Journal of Dental Sciences 18 (2023) 264–271

Available online at www.sciencedirect.com

ScienceDirect

journal homepage: www.e-jds.com

Original Article

Convergent angles of a tapered implant referred from the root profile of premolars

Chung-Chieh Chang [a], Alex Hong [a], Chih-Chun Mei [b], Yi-Fang Huang [c], Heng-Liang Liu [d], I-Ping Lin [e*], Hsiang-Hsi Hong [a**]

[a] *Department of Periodontics, Chang Gung Memorial Hospital Linkou Main Branch and Chang Gung University, Taoyuan City, 333, Taiwan*
[b] *New Taipei City Municipal Tucheng Hospital and Chang Gung University, New Taipei City and Taoyuan City, Taiwan*
[c] *Department of General Dentistry, Chang Gung Memorial Hospital Linkou Main Branch, Taoyuan City, Taiwan*
[d] *Instrument Department, Chang Gung Memorial Hospital Linkou Main Branch, Taoyuan City, Taiwan*
[e] *Division of Periodontology, Department of Dentistry, National Taiwan University Hospital, Hsinchu Branch, Hsinchu, Taiwan*

Received 30 April 2022; Final revision received 26 May 2022
Available online 11 June 2022

KEYWORDS
Tooth root;
Dental implants;
X-ray microtomography;
Biomimetics;
Anatomy

Abstract *Background/purpose:* Limited studies have discussed the convergent profiles regarding tapered implants based on biological considerations. This study analyzed the convergent angles (CAs) of premolar roots and imitated a tapered implant according to the anatomy of tooth roots.

Materials and methods: A total of 60 single-rooted premolars were explored by micro-computed tomography. Every individual root was divided into 10 segments corono-apically, and the roots' buccolingual (BL) and mesiodistal (MD) CAs were measured by sections. To mimic a dental implant, the irregular shape of examined root cross-sections was transformed into a circular shape with equal areas. A biomimetic dental implant (BDI) was reconstructed and its CAs were compared with those of the natural roots' BL and MD at the examined levels and overall estimation.

Results: In general, the maxillary and mandibular premolars demonstrated comparable CA patterns. However, significantly different CA patterns of BL, MD, and BDI were developed for both the maxillary and mandibular roots at the examined levels. The BL's CAs were greater than those CAs measured from the BDI and MD aspects, particularly for the sections at the middle and apical thirds of the roots. For overall CAs, the BDI's CAs were comparable with the average CAs of the BL and MD for both premolar groups.

* Corresponding author. No. 25, Lane 442, Section 1, Jingguo Road, North District, Hsinchu 300, Taiwan
** Corresponding author. 5, Fu-Shin Street, Guishan Dist., Taoyuan City 333, Taiwan
E-mail addresses: iping.lin1123@gmail.com (I.-P. Lin), f1214@cgmh.org.tw (H.-H. Hong).

https://doi.org/10.1016/j.jds.2022.05.022

Conclusion: Instead of a cylindrical configuration, the BDI prototype demonstrated a tapered model with a continuous slope. The average CA of BDI was 14°–24°, serving as a biological reference for future tapered implant design and research.

Introduction

Tapered implants offer certain advantages over cylindrical implants in terms of enhanced primary stability and moderately reduced anatomical restriction.[1] The geometrical shapes of tapered implants vary greatly; some have a continuous slope throughout the body of the fixture, whereas in others, the slope starts from the coronal, middle, or apical third.[2] Because the shape of the implant could influence treatment outcomes, scientists are constantly developing new implant designs to fulfill functional and esthetic demands in various clinical scenarios.[3,4] Application effects of tapered and cylindrical implants have been assessed[5–7]; however, data about the appropriate tapered degree on successful implant treatment is limited.

The consensus on the taper definition in tapered implants was inconclusive. Some studies measured the tapered angle from two sides of the fixtures[8], while others defined it as the angle formed by one side of the fixture and the long axis.[9,10] To clarify the concept, this manuscript applies a convergent angle (CA) to present the observation. CAs have been used to describe tooth preparation of fixed partial dentures[11] and the angle formed by the internal connection of Morse tapered implant and abutment design.[12] The taper slope is used to delineate the angle formed between one side of the tooth root and the tooth axis, and CA is used to depict the angle formed between two sides of the tooth roots.[11] The taper slope/CA concept could also be applied to delineate the implications of tapered fixtures.[13]

The macrostructure of the fixture is associated with the implant's primary stability and biomechanical properties, which are critical for successful implant therapy.[14,15] Some manufacturers design the implant shape mimicking the root form of the natural tooth.[3,16] The rationale behind this could be derived from the biomimetic concept, which is the emulation of natural models to solve complex human problems.[17] Clinicians have applied this concept to restore esthetic implant prostheses and fabricate a root form fixture to accommodate the oral environment.[18,19] Despite the evolution and improvement of tapered implant design, the optimal CA and fixture profile are not well established. A tapered implant CA assessment that correlates with the anatomy of the natural root is recommended.

Tapered implants resembling tooth roots could increase the fixture fitness in the extraction socket during immediate implant placement.[20] Mangano et al. placed root-analogous implants into the extraction sockets of 15 patients and achieved positive primary stability with a minimal marginal bone loss after a year.[16] Hong et al. suggested that tapered implants that imitate premolars had decreased diameters by approximately half in the apical area, which could decrease the risk of apical perforation at the anterior maxilla and facilitate occlusal force transmission.[13] These findings indicate that the development of tapered implants resembling the natural root is promising. Therefore, this study aimed to assess the CAs of premolar roots using micro-computed tomography (μCT) and to correlate the CAs of root anatomy to tapered implants. To simulate a tapered implant, a biomimetic dental implant (BDI) was created by modifying the morphology of premolar roots. Furthermore, CA significances between premolars and BDIs were evaluated. The main goal of this survey was to determine the optimal CA value for a tapered implant based on biological considerations.

Materials and methods

Thirty maxillary and 30 mandibular single-rooted premolars with complete root formation were included in this study, excluding those with cervical or root caries and dilacerated roots. Informed consent was obtained from the patients before tooth extraction. The study protocol followed the principles stipulated in the Declaration of Helsinki and was approved by the Institutional Review Board for Clinical Research at Chang Gung Memorial Hospital (202100902B0).

Teeth were extracted for periodontal or orthodontic causes and cleaned by scaling and root planing to remove calculus and debris. Before scanning, samples were embedded in an acrylic cube along the tooth axis and fixed in formalin solution. Then, the sample was scanned by μCT (SkyScan 1076, Bruker, Kontich, Belgium). The settings for the scanning were as follows: pixel matrix, 2000 × 2000; tube voltage, 100 kV; tube current, 100 μA; and slice thickness, 18 μm, with 10 min of scan time each. The data were exported as digital imaging and communications in medicine (DICOM), generating 1300–1500 sliced images from each tooth.

Tooth measurements

The DICOM files were further converted into standard tessellation language (STL) format using the Mimics Medical software (version 21.0, Materialise NV, Leuven, Belgium). Three-dimensional reconstruction images were manipulated and the CA degrees were measured using the Geomagic Studio 2012 (3D Systems, Rock Hill, SC, USA). A mid-buccolingual (BL) plane was created through the long axis of the tooth. Additionally, two planes perpendicular to the mid-BL plane were created through the root apex and the buccal or lingual cementoenamel junction (CEJ),

respectively. Another nine planes were created between these two planes and parallel to each other, separating the root into 10 equal portions. The 11 planes from the CEJ to the root apex would encounter 11 points on both buccal and lingual sides (Fig. 1a & d). These 22 coordinates could be changed into vectors. The CA of the root could be calculated using the following equation:

$$L1 \cdot L2 = ([L1] \cdot [L2]) \times \cos A$$

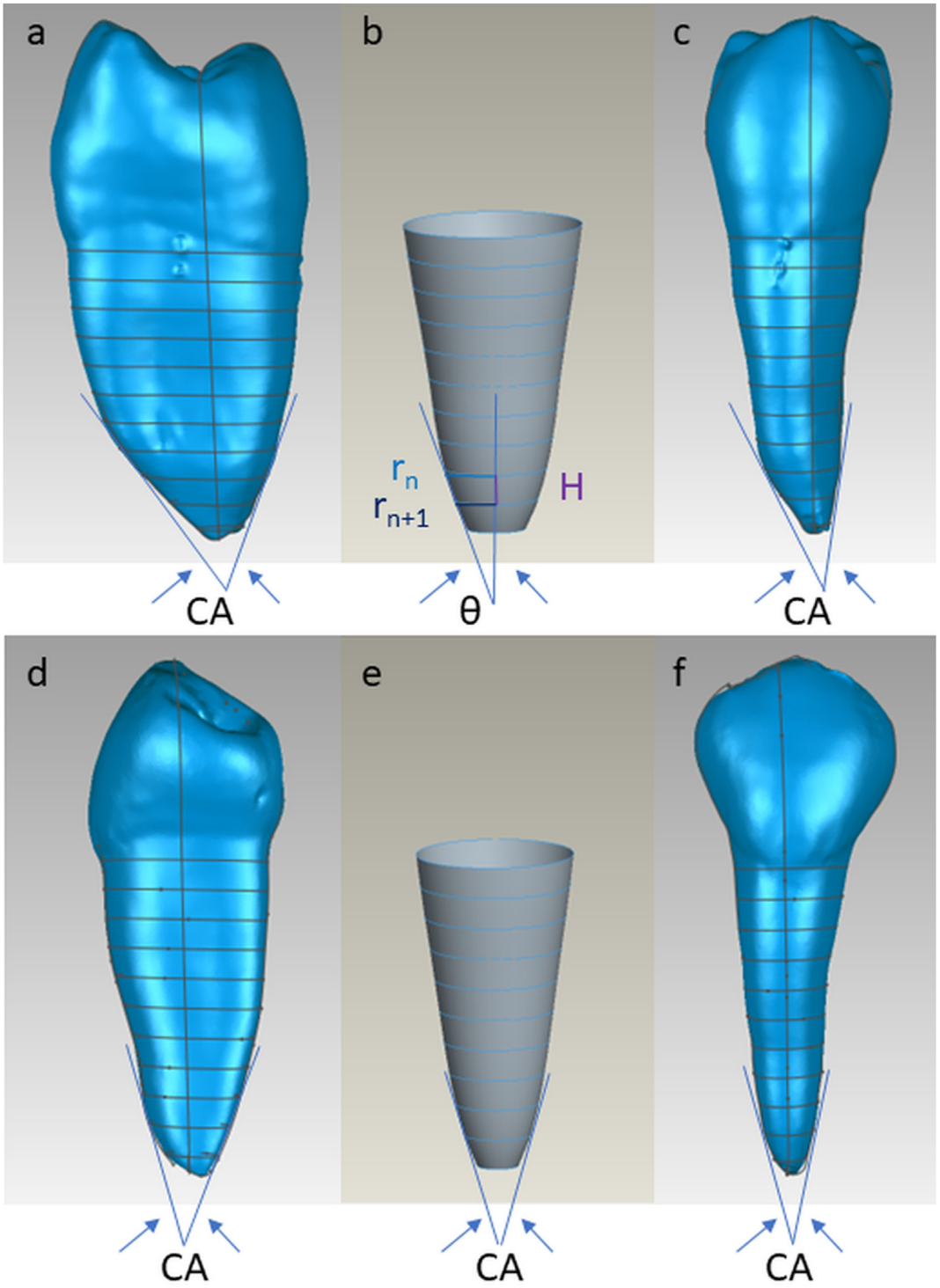

Figure 1 Three-dimensional reconstructions from microcomputed tomography images. a—c: Maxillary premolars; d—f: Mandibular premolars. a & d: Convergent angles (CAs) from the buccolingual measurement. b & e: Transformation of the natural root into a biomimetic dental implant (BDI). r_n: radius of the cross-section at the examined level. r_{n+1}: radius at the next level apical to r_n. H: length of each adjacent slice. θ: angle formed by the long axis and one side of the BDI. c & f: CAs from the mesiodistal measurement.

where L1 is the vector formed by two coordinates of the buccal side, L2 is the vector formed by two coordinates of the lingual side, and A is the CA of the root formed by the BL lines. In this manner, each 10%, 20%, 30%, 40%, and 50% interval of CA from the CEJ to root apex in BL direction was estimated.

An additional mid-mesiodistal (MD) plane through the long axis and root apex was created to measure the CA of the MD aspect. This mid-MD plane would encounter the 11 previously created perpendicular slices, with another 11 coordinates on both the mesial and distal sides (Fig. 1c & f). By changing the coordinate into vectors and using the same equation, CA at each interval (10%, 20%, 30%, 40%, and 50%) from the CEJ to the root apex was estimated in the MD aspect.

The irregular cross-section of the root was transformed into a circular shape from the CEJ to the root apex to mimic a dental implant. The root form of the tooth was converted into the symmetrical conical shape of the BDI (Fig. 1b & e; Online Resource) with the same cross-sectional area from the CEJ to the apex using the following equation:

$$A = \pi r^2$$

where A is the area, π is the circular constant, and r is the radius.

To calculate the CA of the BDI, the following equation was used:

$$\mathrm{Cot}\ \theta = H/(r_n - r_{n+1})$$

where θ is the slope of the taper in the BDI (the angle formed by the long axis and one side of the BDI), CA = 2ɵ, H is the length of each adjacent slice from the CEJ to the apex, r_n is the radius of the cross-section at the examined level, and r_0 and r_{11} are at the levels of the CEJ and apex, respectively. Accordingly, the CA of the BDI from the CEJ to the apex was calculated at each 10%, 20%, 30%, 40%, and 50% interval.

To analyze the overall CAs of the BL, MD, and BDI, the average of each 10% CA from the CEJ to 90% of the root length was used to exclude the most variable part at the root apex. All the measurements were conducted twice with a 2-week interval by an experienced periodontist (C.C.C.).

Statistical analyses

The intraclass correlation coefficient (ICC) was used to calculate the intra-rater reliability. The independent *t*-test was used to compare the CAs between the maxillary and mandibular premolars. One-way analysis of variance was applied to compare the CAs of the BL, MD, and BDI followed by Tukey's honestly significant difference multiple comparisons test. The data analysis was conducted using Statistical Package for Social Sciences software (version 22.0, IBM, Chicago, IL, USA), and the significance level was set at $P < 0.05$.

Results

Tables 1–3 demonstrate the comparisons of the CAs between the maxillary and mandibular premolars in the BL analysis, MD measurement, and transformed CAs of BDI at examined levels. In general, no significant differences in the CAs of BL, MD, and BDI were observed between the maxillary and mandibular roots.

Table 1 Comparisons of the convergent angles (degree) between the maxillary and mandibular premolars in the buccolingual analysis at examined levels.

Examination levels	Maxillary premolars (Mean ± SD)	Mandibular premolars (Mean ± SD)	*P* value
10% interval			
0%–10%	12.10 ± 8.61	10.51 ± 8.83	0.483
10%–20%	10.61 ± 8.18	9.38 ± 7.78	0.553
20%–30%	16.06 ± 9.08	15.24 ± 6.87	0.694
30%–40%	20.92 ± 8.33	17.96 ± 5.60	0.112
40%–50%	23.28 ± 9.75	19.66 ± 6.18	0.092
50%–60%	20.82 ± 8.95	22.37 ± 6.63	0.449
60%–70%	24.79 ± 11.08	23.72 ± 6.27	0.647
70%–80%	31.61 ± 12.31	28.39 ± 12.72	0.324
80%–90%	43.35 ± 16.70	38.66 ± 15.72	0.267
90%–100%	63.02 ± 16.35	61.00 ± 18.17	0.653
20% interval			
0%–20%	11.53 ± 7.25	9.95 ± 7.27	0.402
20%–40%	18.52 ± 8.17	16.63 ± 5.59	0.300
40%–60%	22.13 ± 7.98	21.06 ± 5.20	0.541
60%–80%	28.37 ± 10.37	26.17 ± 8.24	0.368
80%–100%	53.92 ± 15.41	51.66 ± 14.92	0.567
30% interval			
0%–30%	12.97 ± 6.90	11.72 ± 6.70	0.478
30%–60%	21.80 ± 7.25	20.07 ± 4.66	0.277
60%–90%	33.72 ± 12.18	31.02 ± 9.30	0.339
40% interval			
0%–40%	15.00 ± 6.61	13.30 ± 5.92	0.300
40%–80%	25.45 ± 6.87	23.73 ± 4.31	0.250
50% interval			
0%–50%	16.72 ± 6.69	14.61 ± 5.22	0.180
50%–100%	38.17 ± 11.28	36.76 ± 7.87	0.574

Independent *t* test for maxilla vs. mandible.
SD: Standard deviation.

The CAs of BL increased gradually toward the apex for both the maxillary and mandibular premolar roots regardless of the intervals. The CAs of the maxillary and mandibular roots ranged from 10.61° to 63.02°and 9.38°–61.00°, respectively. Insignificant differences were observed among the various examination levels (Table 1). However, the CAs of MD decreased gradually from CEJ to the middle third area, and a continuous increase in CAs developed. Significant CA differences were noted between the maxillary and mandibular groups at the transitional levels (60%–70%; $P = 0.012$, Table 2). In the BDI group, a relatively constant developing pattern of CA from the coronal to the middle third was noted. Subsequently, a greater CA followed toward the apexes for both the maxillary and mandibular BDIs. The CAs ranged from 14.30° to 49.92° for maxillary BDIs and 13.68°–46.85° for mandibular BDIs (Table 3).

Tables 4 and 5 illustrate CA comparisons among BL, BDI, and MD at the maxillary and mandibular arches,

Table 2 Comparisons of the convergent angles (degree) between the maxillary and mandibular premolars in the mesiodistal measurement at examined levels.

Examination levels	Maxillary premolars (Mean ± SD)	Mandibular premolars (Mean ± SD)	*P* value
10% interval			
0%–10%	17.93 ± 8.58	16.55 ± 4.02	0.431
10%–20%	21.24 ± 6.96	20.01 ± 5.95	0.463
20%–30%	20.72 ± 7.67	18.11 ± 4.28	0.111
30%–40%	14.63 ± 8.52	13.93 ± 4.16	0.691
40%–50%	9.44 ± 6.64	10.89 ± 5.29	0.353
50%–60%	8.02 ± 8.01	9.23 ± 5.54	0.496
60%–70%	6.80 ± 5.50	10.82 ± 6.43	0.012*
70%–80%	10.16 ± 5.63	12.81 ± 7.33	0.121
80%–90%	18.29 ± 10.58	19.34 ± 7.44	0.659
90%–100%	33.39 ± 13.02	35.36 ± 15.20	0.591
20% interval			
0%–20%	19.62 ± 7.23	18.31 ± 4.13	0.391
20%–40%	17.64 ± 7.59	16.06 ± 3.35	0.304
40%–60%	8.43 ± 6.13	9.86 ± 5.21	0.335
60%–80%	7.89 ± 4.16	11.62 ± 6.48	0.011*
80%–100%	25.60 ± 11.53	27.83 ± 10.11	0.429
30% interval			
0%–30%	20.08 ± 5.79	18.27 ± 3.56	0.151
30%–60%	10.26 ± 6.42	11.21 ± 4.42	0.507
60%–90%	11.13 ± 5.29	14.32 ± 5.45	0.025*
40% interval			
0%–40%	18.71 ± 5.21	17.22 ± 2.72	0.171
40%–80%	8.23 ± 3.57	10.73 ± 5.19	0.034*
50% interval			
0%–50%	16.82 ± 5.11	15.96 ± 2.38	0.408
50%–100%	15.15 ± 5.28	17.91 ± 5.03	0.043

Independent *t* test for maxilla vs. mandible: *: $P < 0.05$.
SD: Standard deviation.

Table 3 Comparisons of the convergent angles (degree) between the maxillary and mandibular biomimetic dental implants (BDIs) at examined levels.

Examination levels	Maxillary BDIs (Mean ± SD)	Mandibular BDIs (Mean ± SD)	*P* value
10% interval			
0%–10%	14.74 ± 5.54	13.68 ± 3.98	0.396
10%–20%	17.19 ± 5.74	14.95 ± 4.53	0.098
20%–30%	19.36 ± 4.69	16.87 ± 3.28	0.021*
30%–40%	18.23 ± 6.02	16.11 ± 2.86	0.089
40%–50%	17.07 ± 6.98	15.83 ± 3.18	0.382
50%–60%	14.30 ± 6.21	16.09 ± 3.90	0.187
60%–70%	16.73 ± 7.33	17.87 ± 5.71	0.505
70%–80%	24.26 ± 8.64	22.20 ± 7.29	0.321
80%–90%	33.18 ± 12.82	29.39 ± 8.64	0.184
90%–100%	49.92 ± 13.82	46.85 ± 10.99	0.345
20% interval			
0%–20%	15.98 ± 5.28	14.32 ± 3.58	0.161
20%–40%	18.80 ± 5.06	16.50 ± 2.42	0.030*
40%–60%	15.70 ± 5.55	15.97 ± 2.87	0.815
60%–80%	20.55 ± 6.90	20.05 ± 5.79	0.764
80%–100%	41.49 ± 13.19	38.47 ± 8.40	0.294
30% interval			
0%–30%	17.11 ± 4.36	15.18 ± 3.17	0.054
30%–60%	16.55 ± 5.41	16.02 ± 2.58	0.630
60%–90%	24.65 ± 8.20	23.23 ± 5.85	0.443
40% interval			
0%–40%	17.40 ± 4.13	15.41 ± 2.58	0.030*
40%–80%	18.16 ± 4.54	18.03 ± 3.73	0.904
50% interval			
0%–50%	17.34 ± 4.35	15.50 ± 2.23	0.045*
50%–100%	28.13 ± 7.78	26.90 ± 4.73	0.462

Independent *t*-test for maxilla vs. mandible; *: $P < 0.05$.
SD: Standard deviation.

respectively. In general, significant CA differences were observed at the most examined levels corono-apically (except for 20%–40%, 0%–50% at the maxillary roots, and 20%–30%, 20%–40%, 0%–50% at the mandibular roots showed nonsignificantly). In the maxilla, significant CA differences were noted between BL and MD for every 10% consideration. The CAs of BDI did not significantly differ from those of BL and MD at coronal third areas (0%–10%, 20%–40%). However, significant differences in CAs among BL, BDI, and MD were noted from the middle to the apical thirds (Table 4). A similar finding was noted for the mandibular group. Significant CA differences were noted among BL, MD, and BDI at the most examined levels. From the middle thirds to the root apex, all three groups showed significant differences from each other (Table 5).

The overall CAs were generally comparable among the three groups in the maxilla (BL: 22.62° ± 10.12°, BDI: 19.45° ± 5.92°, and MD: 14.14° ± 5.64°; $P = 0.073$; Fig. 2a) and the mandible (BL: 20.21° ± 9.35°, BDI: 18.11° ± 4.85°, and MD: 15.15° ± 4.20°; $P = 0.277$; Fig. 2b). Moreover, an insignificant CA difference was noted between the maxillary and mandibular BL, BDI, and MD ($P = 0.607$, $P = 0.402$, and $P = 0.672$, respectively). The intra-rater reliability for the CA measurements was excellent (ICC: 0.886; 95% confidence interval: 0.810, 0.932).

Discussion

The overall BDI CAs were comparable with the average of the BL and MD CAs of the maxilla and mandible. The average CAs of BDI were 19.45° ± 5.92° in the maxilla and 18.11° ± 4.85° in the mandible, with no significant differences (Fig. 2). Accordingly, the overall CAs of BDI ranging from 14° to 24° could be proposed. The 9° tapered slope of the Straumann® bone level tapered implant at the apical area equals 18° CA, which is comparable to the CAs of this BDI model.[3] Commercial tapered implants typically have a constant CA from the coronal to the middle third and tapered only at the apical third. However, the BDI model, derived from premolar roots, shows different taper CAs at examination levels corono-apically (Table 3). Atieh and Shahmiri investigated the optimal taper for immediately loaded wide-diameter implants. They compared five different tapered implants with slopes ranging from 2° to 14° and discovered that greater taper angles of the implant body increased both stress and strain, indicating that implants with 8° slope (16° CA) may achieve the best results in

Table 4 Convergent angle (CA, degree) comparisons among the buccolingual (BL), biomimetic dental implant (BDI), and mesiodistal (MD) at the maxillary roots.

Examination levels	BL (Mean ± SD)	BDI (Mean ± SD)	MD (Mean ± SD)	*P* value
10% interval				
0–10%	12.10 ± 8.61	14.75 ± 5.54	17.93 ± 8.58	0.017* (MD > BL)
10%–20%	10.61 ± 8.18	17.19 ± 5.74	21.24 ± 6.96	<0.001** (MD, BDI > BL)
20%–30%	16.06 ± 9.08	19.36 ± 4.69	20.72 ± 7.67	0.047* (MD > BL)
30%–40%	20.92 ± 8.33	18.23 ± 6.02	14.63 ± 8.52	0.008** (BL > MD)
40%–50%	23.28 ± 9.75	17.07 ± 6.98	9.44 ± 6.64	<0.001** (BL > BDI > MD)
50%–60%	20.82 ± 8.95	14.30 ± 6.21	8.02 ± 8.01	<0.001** (BL > BDI > MD)
60%–70%	24.79 ± 11.08	16.73 ± 7.33	6.80 ± 5.50	<0.001** (BL > BDI > MD)
70%–80%	31.61 ± 12.31	24.26 ± 8.64	10.16 ± 5.63	<0.001** (BL > BDI > MD)
80%–90%	43.35 ± 16.70	33.18 ± 12.82	18.29 ± 10.58	<0.001** (BL > BDI > MD)
90%–100%	63.02 ± 16.35	49.92 ± 13.82	33.39 ± 13.02	<0.001** (BL > BDI > MD)
20% interval				
0%–20%	11.53 ± 7.25	15.98 ± 5.28	19.62 ± 7.23	<0.001** (MD, BDI > BL)
20%–40%	18.52 ± 8.17	18.80 ± 5.06	17.64 ± 7.59	0.804
40%–60%	22.13 ± 7.98	15.70 ± 5.55	8.43 ± 6.13	<0.001** (BL > BDI > MD)
60%–80%	28.37 ± 10.37	20.55 ± 6.90	7.89 ± 4.16	<0.001** (BL > BDI > MD)
80%–100%	53.92 ± 15.41	41.49 ± 13.19	25.60 ± 11.53	<0.001** (BL > BDI > MD)
30% interval				
0%–30%	12.97 ± 6.90	17.11 ± 4.36	20.08 ± 5.79	<0.001** (MD, BDI > BL)
30%–60%	21.80 ± 7.25	16.55 ± 5.41	10.26 ± 6.42	<0.001** (BL > BDI > MD)
60%–90%	33.72 ± 12.18	24.65 ± 8.20	11.13 ± 5.29	<0.001** (BL > BDI > MD)
40% interval				
0%–40%	15.00 ± 6.61	17.40 ± 4.13	18.71 ± 5.21	0.03* (MD > BL)
40%–80%	25.45 ± 6.87	18.16 ± 4.54	8.23 ± 3.57	<0.001** (BL > BDI > MD)
50% interval				
0%–50%	16.72 ± 6.69	17.34 ± 4.35	16.82 ± 5.11	0.894
50%–100%	38.17 ± 11.28	28.13 ± 7.78	15.15 ± 5.28	<0.001** (BL > BDI > MD)

One-way ANOVA for comparison between CA of each group and followed by post-hoc Tukey HSD.
* $P < 0.05$, **: $P < 0.01$; SD: Standard deviation.

healed sites in terms of stress minimization around the implant neck.[8] The encouraging biomechanical data of a tapered implant with 16° CA, which is consistent with our BDI model, supported the hypothesis that a tapered implant mimicking root form might exhibit a better stress distribution pattern. However, Petrie and Williams evaluated the effect of implant design on strain in the alveolar crest and discovered that their tapered samples could enhance crestal strain without considering the interactive effect of implant diameter, length, and taper design on crestal bone strain.[9] Despite several studies evaluating the effects of varied CAs on the clinical and research performance of tapered implants, further research is required to examine the biomechanical properties and primary stability of these BDI models to enhance CA knowledge of tapered implants.

Limited studies have evaluated the CAs of tooth roots and the association correlated with those of tapered implants.[13,21] With the benefits of μCT, the CAs of premolar roots can be measured precisely in various directions and sections. Fantozzi et al. analyzed the root morphology of anterior teeth in Europeans using a millimeter gauge to evaluate the root taper extraorally in the vestibular–oral (VO) and MD directions.[21] Three different landmarks at the coronal, middle, and apical thirds were defined, and the diameters of each landmark were measured. Tapering percentage expressed the root tapering and defined the reduction of the two diameters from three different levels to calculate the coronal, apical, and overall root tapering. A substantial and progressive root tapering was observed in the VO and MD directions. However, our results only supported an increased tendency of CA in the BL measurement (Table 1). The various findings between these two studies might be attributed to the selected type of teeth (anterior teeth vs. premolars), different landmarks, and measurement tools used (millimeter gauge vs. μCT and software).

From the BL aspect, CAs increased gradually from CEJ to the apex for both arches premolars in this study (Table 1), which could be initiated by the shift from a relatively straight profile to a pointed profile on the BL direction of the root (Fig. 1a & d). By contrast, CAs at the MD side decreased gradually followed by a subsequent increase (Table 2). A high prevalence of root concavities on premolars at the mesial and/or distal sides could elucidate the funnel-like appearance.[22] A relatively constant CA value of BDI was observed at coronal 2/3, followed by a gradual CA increase toward the apex (Table 3). The amount of the cross-section areas that was consistently reduced coronoapically accounted for the relatively constant CA values of the maxillary and mandibular BDI. The greater CA at the apical third also supports the tapered design at the apical third for some implant systems.[23] An insignificant difference in BL, BDI, and MD was observed between the

Table 5 Convergent angle (CA, degree) comparisons among the buccolingual (BL), biomimetic dental implant (BDI), and mesiodistal (MD) at the mandibular roots.

Examination levels	BL (Mean ± SD)	BDI (Mean ± SD)	MD (Mean ± SD)	*P* value
10% interval				
0%–10%	10.51 ± 8.83	13.68 ± 3.98	16.55 ± 4.02	0.001** (MD > BL)
10%–20%	9.38 ± 7.78	14.95 ± 4.53	20.01 ± 5.95	<0.001** (MD > BDI > BL)
20%–30%	15.24 ± 6.87	16.87 ± 3.28	18.74 ± 4.28	0.091
30%–40%	13.93 ± 4.16	16.11 ± 2.86	17.96 ± 5.60	0.002** (MD > BL)
40%–50%	19.66 ± 6.19	15.83 ± 3.18	10.89 ± 5.29	<0.001** (BL > BDI > MD)
50%–60%	22.37 ± 6.63	16.09 ± 3.90	9.23 ± 5.54	<0.001** (BL > BDI > MD)
60%–70%	23.72 ± 6.27	17.87 ± 5.71	10.82 ± 6.43	<0.001** (BL > BDI > MD)
70%–80%	28.39 ± 12.72	22.20 ± 7.29	12.81 ± 7.33	<0.001** (BL > BDI > MD)
80%–90%	38.65 ± 15.72	29.39 ± 8.64	19.34 ± 7.44	<0.001** (BL > BDI > MD)
90%–100%	61.00 ± 18.17	46.85 ± 10.99	35.36 ± 15.20	<0.001** (BL > BDI > MD)
20% interval				
0%–20%	9.95 ± 7.27	14.32 ± 3.58	18.31 ± 4.13	<0.001** (MD > BDI > BL)
20%–40%	16.63 ± 5.59	16.50 ± 2.42	16.06 ± 3.35	0.851
40%–60%	21.06 ± 5.20	15.97 ± 2.87	9.86 ± 5.21	<0.001** (BL > BDI > MD)
60%–80%	26.17 ± 8.24	20.05 ± 5.79	11.62 ± 6.48	<0.001** (BL > BDI > MD)
80%–100%	51.66 ± 14.92	38.47 ± 8.40	27.83 ± 10.11	<0.001** (BL > BDI > MD)
30% interval				
0%–30%	11.72 ± 6.70	15.18 ± 3.17	18.27 ± 3.56	<0.001** (MD > BDI > BL)
30%–60%	20.07 ± 4.66	16.02 ± 2.58	11.21 ± 4.42	<0.001** (BL > BDI > MD)
60%–90%	31.02 ± 9.30	23.23 ± 5.85	14.32 ± 5.45	<0.001** (BL > BDI > MD)
40% interval				
0%–40%	13.30 ± 5.92	15.41 ± 2.58	17.22 ± 2.72	0.001** (MD > BL)
40%–80%	23.73 ± 4.31	18.03 ± 3.73	10.73 ± 5.19	<0.001** (BL > BDI > MD)
50% interval				
0%–50%	14.61 ± 5.22	15.50 ± 2.23	15.96 ± 2.38	0.333
50%–100%	36.76 ± 7.87	26.90 ± 4.73	17.91 ± 5.03	<0.001** (BL > BDI > MD)

One-way ANOVA for comparison between CA of each group and followed by post-hoc Tukey HSD.
*: $P < 0.05$, **: $P < 0.01$; SD: Standard deviation.

maxillary and mandibular CAs (Tables 1–3); therefore, it is feasible to install a tapered implant with a consistent CA at both maxillary and mandibular premolar areas.

At individual examination levels, most BL, BDI, and MD CAs showed significant differences in both the maxilla and mandible (Tables 4 and 5). The MD CA was significantly different from the BL CA, which was related to dimensional differences at the cross-sectional levels of the root. A wider BL dimension at the coronal third accounted for the greater CAs at the middle and apical thirds of the roots. Another study also supported greater BL dimensions at three measured levels in the anterior teeth.[21] Unlike natural roots, BDI showed a

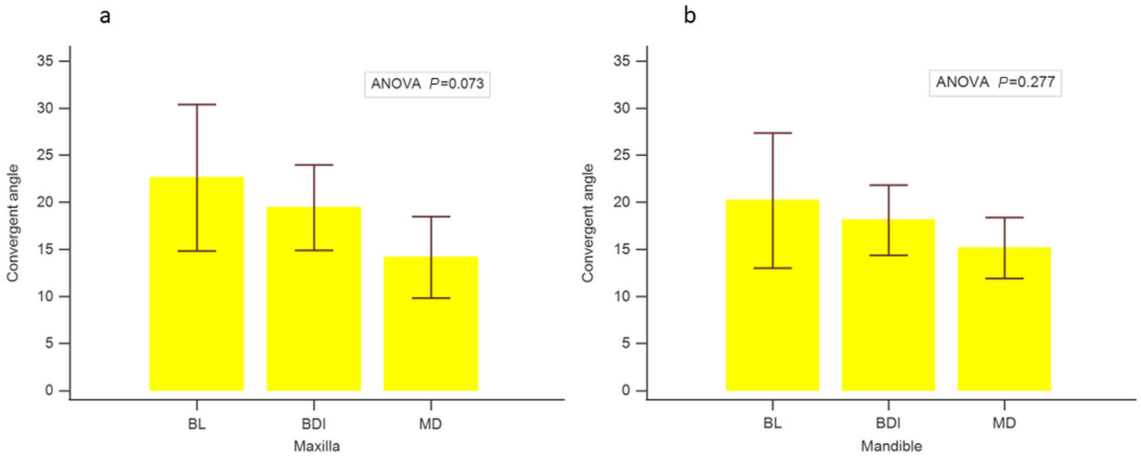

Figure 2 Comparison of the overall convergent angles between the buccolingual (BL) and mesiodistal (MD) direction and the biomimetic dental implant (BDI). a: Maxillary premolars. b: Mandibular premolars.

relatively consistent CA, particularly at the coronal two-thirds. Transformed CAs referred from decreased BL and increased MD dimensions partially explain the findings (Fig. 1). The interproximal root concavities and irregular cross-sectional contours of premolar roots might account for the variations in CA in the BL and MD measurements.

The limitations of this study are as follows. Only premolars were included, and the sample size was small. Studies on other types of teeth, such as incisor, canine, and single-rooted molars, are required to have a comprehensive insight into the taper of natural roots. Moreover, the measurements were performed on natural teeth only. Future investigations are needed to explore the CAs of different tapered implants and compare their biomechanical properties with those of the tooth roots.

In conclusion, this study provides a biological rationale for the CA design of the tapered implants. The CAs of the BDI derived from the premolar roots ranged from 14° to 24°, which were comparable with the average CAs of the buccolingual and mesiodistal aspects of premolar roots for both arches. The information of the CAs of BDIs could not only assist researchers to investigate proper tapered implant design, but also aid clinicians to select an optimally designed implant fixture in daily practice.

Declaration of competing interest

The authors have no conflicts of interest relevant to this article.

Acknowledgments

The study protocol was approved by an Institutional Review Board for Clinical Research in Chang Gung Memorial Hospital (No. 202100902B0) and the study was supported by Chang Gung Memorial Hospital (CMRPG3M0331).

Appendix A. Supplementary data

Supplementary data to this article can be found online at https://doi.org/10.1016/j.jds.2022.05.022.

References

1. Alves CC, Neves M. Tapered implants: from indications to advantages. *Int J Periodontics Restor Dent* 2009;29:161—7.
2. Jokstad A, Ganeles J. Systematic review of clinical and patient-reported outcomes following oral rehabilitation on dental implants with a tapered compared to a non-tapered implant design. *Clin Oral Implants Res* 2018;29(Suppl 16):41—54.
3. Dard M, Kuehne S, Obrecht M, Grandin M, Helfenstein J, Pippenger BE. Integrative performance analysis of a novel bone level tapered implant. *Adv Dent Res* 2016;28:28—33.
4. Emmert M, Gülses A, Behrens E, et al. An experimental study on the effects of the cortical thickness and bone density on initial mechanical anchorage of different Straumann® implant designs. *Int J Implant Dent* 2021;7:1—8.
5. Kadkhodazadeh M, Heidari B, Abdi Z, Mollaverdi F, Amid R. Radiographic evaluation of marginal bone levels around dental implants with different designs after 1 year. *Acta Odontol Scand* 2013;71:92—5.
6. Sanz M, Cecchinato D, Ferrus J, Pjetursson EB, Lang NP, Lindhe J. A prospective, randomized-controlled clinical trial to evaluate bone preservation using implants with different geometry placed into extraction sockets in the maxilla. *Clin Oral Implants Res* 2010;21:13—21.
7. Ellis R, Chen S, Davies H, Fitzgerald W, Xu J, Darby I. Primary stability and healing outcomes of apically tapered and straight implants placed into fresh extraction sockets. A pre-clinical in vivo study. *Clin Oral Implants Res* 2020;31:705—14.
8. Atieh MA, Shahmiri RA. Evaluation of optimal taper of immediately loaded wide-diameter implants: a finite element analysis. *J Oral Implantol* 2013;39:123—32.
9. Petrie CS, Williams JL. Comparative evaluation of implant designs: influence of diameter, length, and taper on strains in the alveolar crest. A three-dimensional finite-element analysis. *Clin Oral Implants Res* 2005;16:486—94.
10. Didier P, Piotrowski B, Le Coz G, Joseph D, Bravetti P, Laheurte P. Finite element analysis of the stress field in peri-implant bone: a parametric study of influencing parameters and their interactions for multi-objective optimization. *Appl Sci* 2020;10:5973.
11. Al-Moaleem MM, Shariff M, Porwal A, AlMakhloti EA, Tikare S. Evaluation of the degree of taper and convergence angle of full ceramo-metal crown preparations by different specialists centers at Assir Region, Saudi Arabia. *Saudi J Med Med Sci* 2015;3:198—203.
12. Pita MS, Anchieta RB, Barão VA, Garcia Jr IR, Pedrazzi V, Assunção WG. Prosthetic platforms in implant dentistry. *J Craniofac Surg* 2011;22:2327—31.
13. Hong HH, Hong A, Chang CC, Liu HL, Mei CC. Characteristics of the convergent angles of tapered implants based on a premolar root model. *J Prosthet Dent* 2021.
14. Falco A, Berardini M, Trisi P. Correlation between implant geometry, implant surface, insertion torque, and primary stability: in vitro biomechanical analysis. *Int J Oral Maxillofac Implants* 2018;33:824—30.
15. Wilson Jr T, Miller R, Trushkowsky R, Dard M. Tapered implants in dentistry: revitalizing concepts with technology: a review. *Adv Dent Res* 2016;28:4—9.
16. Mangano FG, De Franco M, Caprioglio A, Macchi A, Piattelli A, Mangano C. Immediate, non-submerged, root-analogue direct laser metal sintering (DLMS) implants: a 1-year prospective study on 15 patients. *Laser Med Sci* 2014;29:1321—8.
17. Vincent JF, Bogatyreva OA, Bogatyrev NR, Bowyer A, Pahl AK. Biomimetics: its practice and theory. *J R Soc Interface* 2006;3:471—82.
18. Mandelli F, Ghensi P, Traini T. Biomimetic implant restoration made of human enamel and CAD/CAM block: a short report. *Quintessence Int* 2019;50:330—3.
19. Pirker W, Kocher A. Immediate, non-submerged, root-analogue zirconia implants placed into single-rooted extraction sockets: 2-year follow-up of a clinical study. *Int J Oral Maxillofac Surg* 2009;38:1127—32.
20. Westover B. Three-dimensional custom-root replicate tooth dental implants. *Oral Maxillofac Surg Clin North Am* 2019;31:489—96.
21. Fantozzi G, Leuter C, Bernardi S, Nardi GM, Continenza MA. Analysis of the root morphology of European anterior teeth. *Ital J Anat Embryol* 2013;118:78—91.
22. Zhao H, Wang H, Pan Y, Pan C, Jin X. The relationship between root concavities in first premolars and chronic periodontitis. *J Periodontal Res* 2014;49:213—9.
23. Gehrke SA, Pérez-Albacete Martínez C, Piattelli A, Shibli JA, Markovic A, Calvo Guirado JL. The influence of three different apical implant designs at stability and osseointegration process: experimental study in rabbits. *Clin Oral Implants Res* 2017;28:355—61.